

Dynamic behaviour of a flexible membrane tsunami Barrier with Dyneema®

Hofland, Bas; Marissen, Roel; Bergsma, Otto

Publication date

2016

Document Version

Accepted author manuscript

Published in

Proceedings of Coastal Structures & Solutions to Coastal Disasters Joint Conference

Citation (APA)

Hofland, B., Marissen, R., & Bergsma, O. (2016). Dynamic behaviour of a flexible membrane tsunami Barrier with Dyneema®. In *Proceedings of Coastal Structures & Solutions to Coastal Disasters Joint Conference*

Important note

To cite this publication, please use the final published version (if applicable). Please check the document version above.

Copyright

Other than for strictly personal use, it is not permitted to download, forward or distribute the text or part of it, without the consent of the author(s) and/or copyright holder(s), unless the work is under an open content license such as Creative Commons.

Takedown policy

Please contact us and provide details if you believe this document breaches copyrights. We will remove access to the work immediately and investigate your claim.

Dynamic behaviour of a flexible membrane tsunami Barrier with Dyneema®

Bas Hofland¹, Roelof Marissen^{2,3}, and Otto Bergsma³

¹Deltares, Boussinesqweg 1, Delft, The Netherlands. bas.hofland@deltares.nl.

²DSM Dyneema, Urmond, The Netherlands.

³Delft University of Technology, Faculty of Aerospace Engineering, Delft, The Netherlands.

ABSTRACT

Proof-of-concept model tests on a novel self-deploying on-shore tsunami barrier were executed. The tsunami barrier consists of a membrane, floater and cables that are stored underground. Due to buoyancy the barrier self-deploys when struck by a tsunami. The membrane and cables consist of the strong, flexible and light-weight material Dyneema® that can resist a 20 m high water column. A novel tsunami generating method was applied to generate a high-velocity initial bore, followed by a long duration high water level, using a normal piston type wave maker in a wave flume. Numerical calculations using a numerical Volume-of-Fluid code were used to tune the tsunami generation. The tests showed that the tsunami barrier indeed automatically deployed and completely blocked a 19 m high (reflected) tsunami for bore velocities up to 7.5 m/s. For higher bore velocities the barrier still deployed. For larger tsunamis (with a 33 m reflected water depth) the barrier remained erected, although overflow evidently occurred.

INTRODUCTION

Since the occurrence of recent tsunamis (Thailand 2004, Tohoku 2011), tsunamis are well known events. They are very long waves generated by rare events like earthquakes, landslides, or meteorite impacts. When a tsunami wave approaches the coast, the wave celerity decreases, and the wave height increases.

At the moment large parts of Japan are protected by roughly 10 m high walls, and the construction has begun of a great wall, with total costs estimated at roughly ten billion dollars. This wall has to be able to stop a Level 1 tsunami, occurring once per several decades to a hundred years. The wall can overflow, but should not collapse, for a Level 2 tsunami, that occurs about every thousand years. The typical height of a Level 1 tsunami wall is 10 m and the typical height of a Level 2 tsunami wall is 15 m or more.

The large concrete tsunami protection walls cause a large obstruction to the access to the sea. Therefore temporary barriers are applied. Preferably these temporary barriers are self-deploying, as during the 2011 tsunami many steel flood gates could not be closed in time. In Japan several temporary tsunami barriers that are erected when a tsunami is predicted have been developed, like flap-type barriers (Kimura et al., 2013), or a pile-type barrier, or steel gates.

In this paper a self-deploying tsunami barrier with Dyneema[®] is studied experimentally. The main aim is to show that the automatic deployment of the barrier functions. To this end physical model tests were executed. A (to the authors' knowledge) new method to study generate tsunami attack on a fully blocking coastal barrier was used. The use of the technique is explained.

The paper is structured as follows. First the material Dyneema[®] and the barrier are described. Next the theory of the membrane shape under hydrodynamic loading is described. Then the experimental setup is described, with an explanation of the new tsunami generating method. Then the results of the tests are described and discussed, and an indication of the forces on the structure is given. Lastly conclusions and recommendations are given.

FLEXIBLE MEMBRANE TSUNAMI BARRIER WITH DYNEEMA[®]

The barrier is located on shore. It is stored with a folded membrane in a trench such that it does not form a (visual) obstruction of the coastline when inactive. Once a tsunami occurs it automatically deploys due to buoyancy. It is preferable to locate the barrier on shore, as it enables easy construction and maintenance. Depending on the shape of the coastline, a tsunami can show several shapes, like a bore (turbulent water front), a series of smaller waves, or a slowly varying water level. However, onshore the hydrodynamic attack is expected to be a more predictable run-up type flow attack, for which it is easier to predict and thus guarantee the deployment of the barrier.

Dyneema[®] is a highly orientated ultra-high molecular weight polyethylene fiber with a very high tensile strength of 3400 MPa and a mass density comparable to water of 975 kg/m³ (Marissen, 2011). The material has a large tear resistance. It also has a very high axial modulus of about 120 GPa. The fracture strain is in the order of 3%, while the bending stiffness is very low. It is used in demanding applications in the fields like offshore, maritime, defence, aviation and safety. This fiber can be woven and impregnated with a polyethylene resin, resulting in a very strong membrane (Marissen *et al.* 2013).

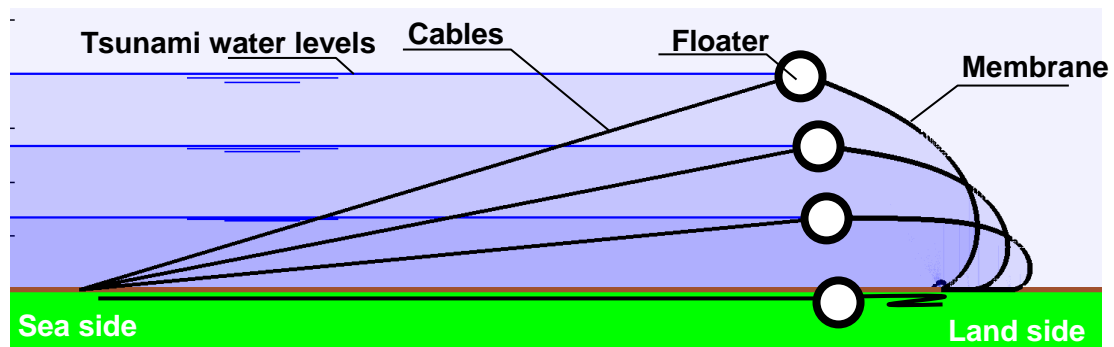


Figure 1. Tsunami barrier with several water levels.

To utilize the strength of this fiber in a flood barrier, the main part of the barrier must be loaded by tension. To this end the Tsunami Barrier with Dyneema[®] was devised. The barrier consists of a floater that is connected to a Dyneema[®] membrane and

cables, see Figure 1. The buoyancy on the floater is balanced by the tension in cables and membrane. It was calculated that a 20 m static water column can be balanced with a 6 mm thick Dyneema[®] membrane with a safety factor of 2 (Marissen *et al.*, 2013).

However, the opening process of the barrier under more realistic, dynamic tsunami loading had not been studied. Therefore a tsunami had to be modelled. It was required to model both the high-intensity approach flow of the initial tsunami impact, as well as the long duration high water level that follows. In the next section, first some considerations about the membrane shape during the barrier opening process are given.

Quasi-static membrane shape during rising water levels. The membrane can only be loaded by tension. Therefore it can only take a horizontal hydrostatic load if the hydrostatic pressure is balanced by the curvature of the tensioned membrane, or:

$$\frac{d\theta}{ds} = \frac{T}{p} \quad (1)$$

The symbols and the principle are defined in Figure 2. The calculations of the membrane shape and forces are described by Marissen *et al.* (2013). Here the membrane angle at the bottom is taken as a starting point, and by solving eq. (1) numerically, the resulting shape is calculated, until the surface is reached. In Marissen *et al.* (2013) only angles at the bottom larger than zero were regarded.

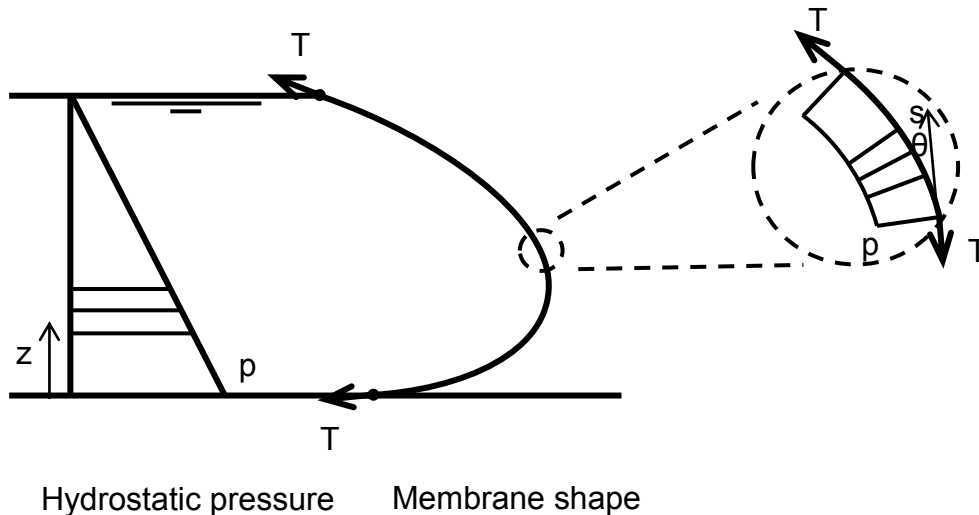


Figure 2. Tsunami barrier membrane shape, symbol definitions.

However, when looking at the possible solutions it was found that for low water levels, the initial angle of the solution of eq. (1) at the bottom is zero. In this case first part of the membrane can be lying flat on the floor, before the part of the membrane starts where eq. (1) applies, and a solution for a fixed membrane size can be found for any intermediate depth. This can be seen for the lower water depths in

Figure 1. In this figure the calculated membrane profiles are depicted for a membrane length of 30 m, a cable length of 70 m and water depths of 0 m, 7.3 m, 14.7 m, and 20 m.

TSUNAMI GENERATING METHOD

Often-used models for tsunamis are solitons, although these are far from perfect models for a real tsunami (Madsen *et al.*, 2008). Also N-waves (Tadepalli and Synolakis, 1994) are often used to include a leading trough. In (large) wave flumes with piston type wave makers these solitons or N-waves can be generated, but a typical very long duration of the tsunami usually cannot be made with the available limited stroke. Long-duration tsunamis are often generated by a large wave paddle, or pneumatic wave maker (e.g. Rosetto *et al.*, 2010) at very small scale. Sometimes a stationary flow is used to model the long-duration part of an overflowing tsunami (Arikawa *et al.*, 2012; Esteban *et al.*, 2014), or a dambreak flow is initiated to model the initial impact (Fulmi *et al.*, 1963).

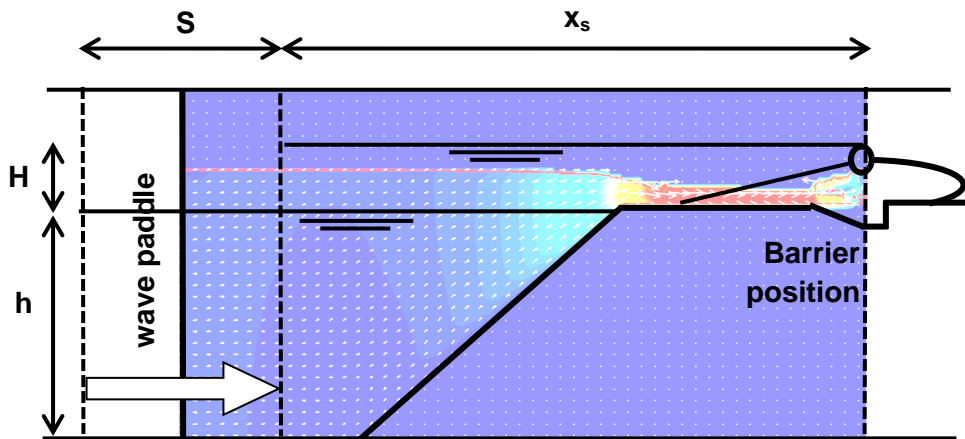


Figure 3. Schematic overview of model setup for tsunami generation.

For the present experiments it was required to test the tsunami barrier on its ability to unfold during a range of realistic tsunami conditions. To this end we needed a synthetic model tsunami that has two characteristics. Firstly a high-velocity bore-type approach flow should be generated. Secondly, a long duration high water level should be present after this initial water level rise. This had to be executed at a reasonable scale with limited effort (i.e. in an existing wave flume), which was not possible with above mentioned methods. It was thought possible to accomplish this by placing the structure close to a large-stroke piston type wave paddle. Only a short foreshore then has to be applied. In this way a permanently increased water level can be obtained, after an initial bore-like impact.

The principle of the method is depicted in Figure 3. The structure to be tested is placed on a short and high foreshore, close to the wave paddle. In case of a fully blocking barrier the static water level that can be attained can be determined by simple volume conservation:

$$H = \frac{S h}{x_s} \quad (2)$$

The symbols are explained in Figure 3. From eq. (2) it is clear that the final water level of the tsunami depends on stroke, distance of the barrier to the paddle, and of the height of the foreshore (offshore water depth).

The speed (distribution) at which the piston is pushed forward and the shape of the foreshore will determine the final shape of the tsunami. The wave steering signal was made by the Goring and Raichlen (1980) method. For any long transient wave (train) with assumed constant celerity and constant shape the paddle position, X , as function of time can be described as:

$$X(t) = \int_{-\infty}^t \frac{c \cdot \eta(X, t')}{h + \eta(X, t')} dt' \quad (3)$$

where c is the celerity of the transient wave, $\eta(x,t)$ the required water surface elevation at location x and time t , and h the water depth. Using this relation, the paddle motion can easily be determined with an explicit numerical integration. The theoretical target water surface $\eta(x)$, consisted of a tanh-shape of required width followed by an elevated water level of infinite length, see the solid line in Figure 4. This shape is assumed to move unaltered with the soliton celerity, c , which is used in eq. (3).

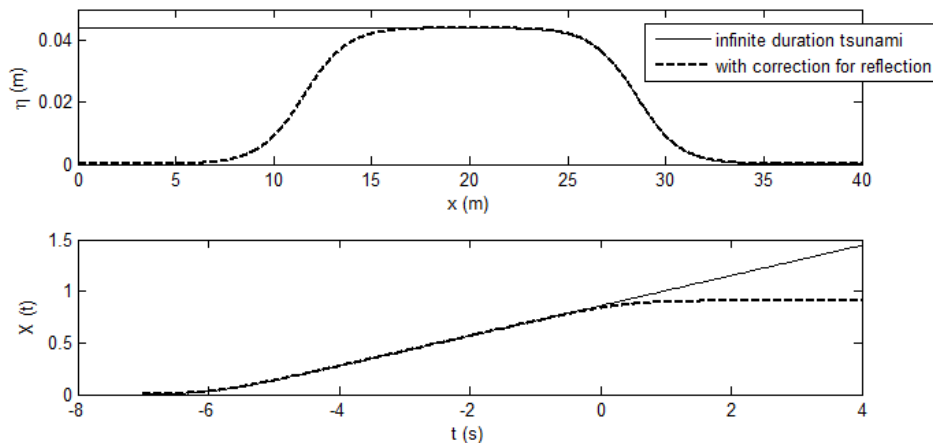


Figure 4. Target wave shape and wave paddle motion ($H=0.2\text{m}$ and $u=7.5\text{m/s}$).

The Active Reflection Compensation system (ARC) on the wave paddle, that works very well for short waves, has not been developed to operate on infinitely long waves, as applied presently. Therefore the reflections of the tsunami wave were augmented by stopping the paddle motion at the stroke as calculated by eq. (2), by applying another tanh-shape to the wave. The timing and width of this shape can be determined theoretically, or the ARC system can be adapted. However, for the

present study a trial and error approach was used. The resulting steering signal is given by the dashed line in Figure 4. The first optimizations of the wave paddle motion were evaluated using a numerical model, which is described next.

Comflow calculations. The tsunami generation method was verified and optimized by numerical simulations with the Volume-of-Fluid numerical model Comflow. See Figure 5 for some snapshots. The wave maker was introduced by a moving block, and the tsunami barrier was modelled by a vertical wall. The computational grid contained $2 \cdot 10^4$ grid cells, and a typical calculation took 2 hours on a normal laptop.

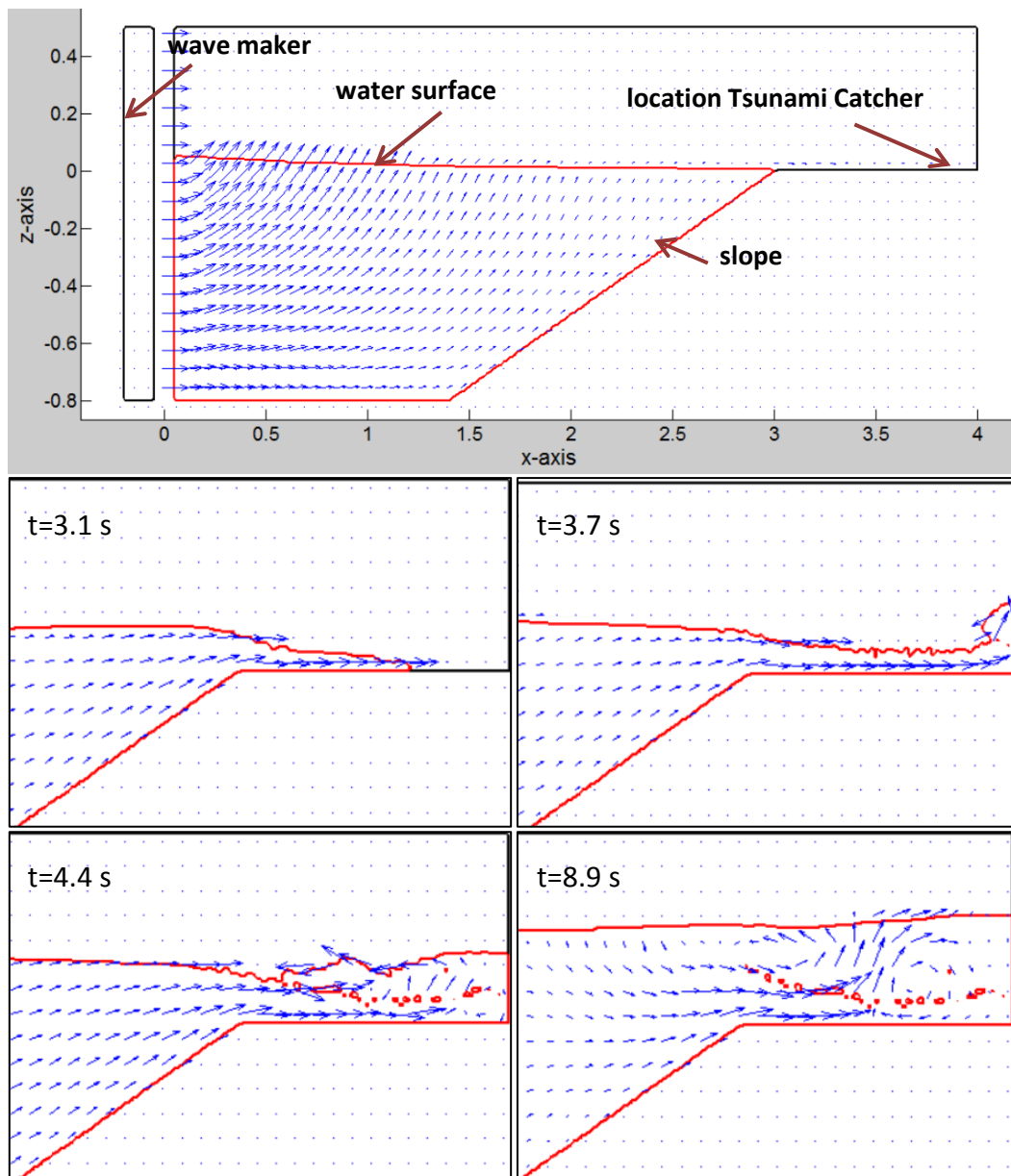


Figure 5. Tsunami attack on vertical tsunami barrier in numerical model

Forces on a vertical wall, as calculated by the model are expected to be an upper bound for the forces on the flexible barrier. These forces on a vertical (model barrier) were evaluated. They are treated later in this paper.

EXPERIMENTS

Setup. Several proof-of-concept experiments were done in the Scheldt Flume of Deltares, Delft. A typical model scale of 1:100 was applied. The glass-walled flume is 1 m wide and 1.2 m deep. The powerful wave paddle has a full stroke of 2 m.

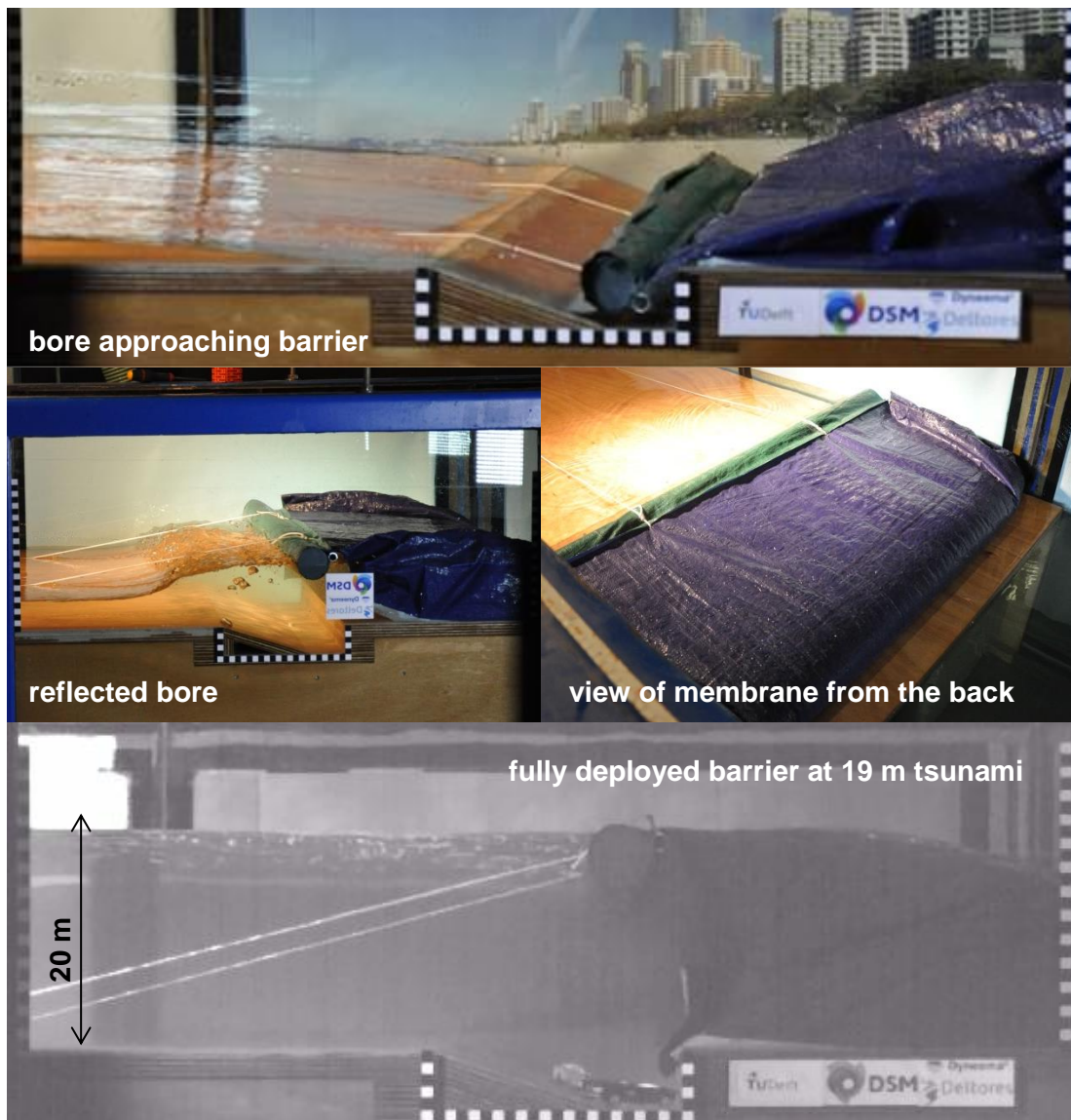


Figure 6. Tsunami attack on tsunami barrier in physical model (pictures mirrored for consistency).

The modelled tsunami barrier was made of a flexible polyethylene membrane. A hollow foam tube was used as a floater, and the cables were made from Dyneema[®]. It

was placed on a wooden foreshore of 0.8 m high, a 1:2 slope, and with a 1.44 m distance from the coastline to the floater. The modelled membrane is 70 m wide (cross shore direction) and fixated to the ground downstream of the floater. The floater is placed under ground in a 5 m deep cavity. The membrane was placed flat downstream of the floater. In reality it will be stored folded in the cavity as well.

The basic tests were done with the following settings (model scale). The stroke $S = 1$ m, $x_s \approx 4$ m (to end of membrane), floater at 3.65 m from the fully extended wave paddle. The initial water depth was $h = 0.8$ m. With these values, eq. (3) predicts a final tsunami level of $H = 0.2$ m. The extreme wave was made with $S = 2$ m, leading to the expected H of 0.4 m. For this test a hole was made in the slope, and the piston was slowly pulled backward (several minutes), letting the water level in front of the foreshore level out. This led to a slightly reduced water level, and a slow lowering of the extreme water level, due to the same hole.

The wave motion was filmed by a (high-speed) camera, and by normal camera. Black-and white markers of 1 cm length are placed around the cavity in which the floater was located.

Test programme. The basic test setup was tested with 36 tests. The following variations were tested (prototype, non-down scaled values are given):

- Cable length: 72 and 144 m.
- Cable attachment: at bottom, middle and top of floater.
- Floater size: 4 and 5 m.
- Velocity of tsunami: 7.5, 10, and 11 m/s.
- Height of tsunami: 19 m and 33 m.

Most tests were executed with the model tsunami with representing a 7.5 m/s flow velocity, and 19 m height.

RESULTS AND OBSERVATIONS

An iterative approach was applied to obtain good boundary conditions. The exact timing of the wave paddle was adjusted in order to minimize the sloshing motion of the water level after the highest water level was reached. The approach flow characteristics were obtained from the video recordings: bore-tip velocity u (when reaching the cavity), and highest tsunami level H .

The wave behaviour was as expected from the numerical calculations. The cavity in the ground did not influence the overall flow. The velocity of the initial wave was optimized such that the paddle approximately stopped when the reflected wave reached the wave paddle. In this way the seiching motion of the flume after wave generation was minimized to one or two metres (cm in model). The barrier deployed in all tests.

The model setup with a 72 m cable, 4 m floater diameter, and cable attachment at the middle of the floater was sufficient to fully block the 19 m high and 7.5 m/s fast flow. No water was seen to spill over the floater. For the 10 m/s approach flow velocity some overtopping occurred after the initial impact, but the barrier still deployed. The occurring velocity under realistic tsunami attack still has to be

determined, but will depend on the specific tsunami, and shoreline shape and bathymetry.

The cavity shape was optimized. It was made both square and with a 1:2 upstream slope. The slope functioned much better, as the floater was pushed up by the flow – instead of pushed down initially (see top pictures in Figure 7).

With the cables connected to the middle of the floater, the barrier erected faster than with the cable connected to the top or bottom of the floater, as indicated in the middle pictures in Figure 7.

The shorter (72 m long) cables create a larger downward force component than the longer (144 m long) cables, such that the floater lies deeper in the water. This is indicated in the bottom pictures in Figure 7. It fully stopped the $H = 19 \text{ m}$ / $u = 7.5 \text{ m/s}$ tsunami, and no clear difference was observed between rising velocities.

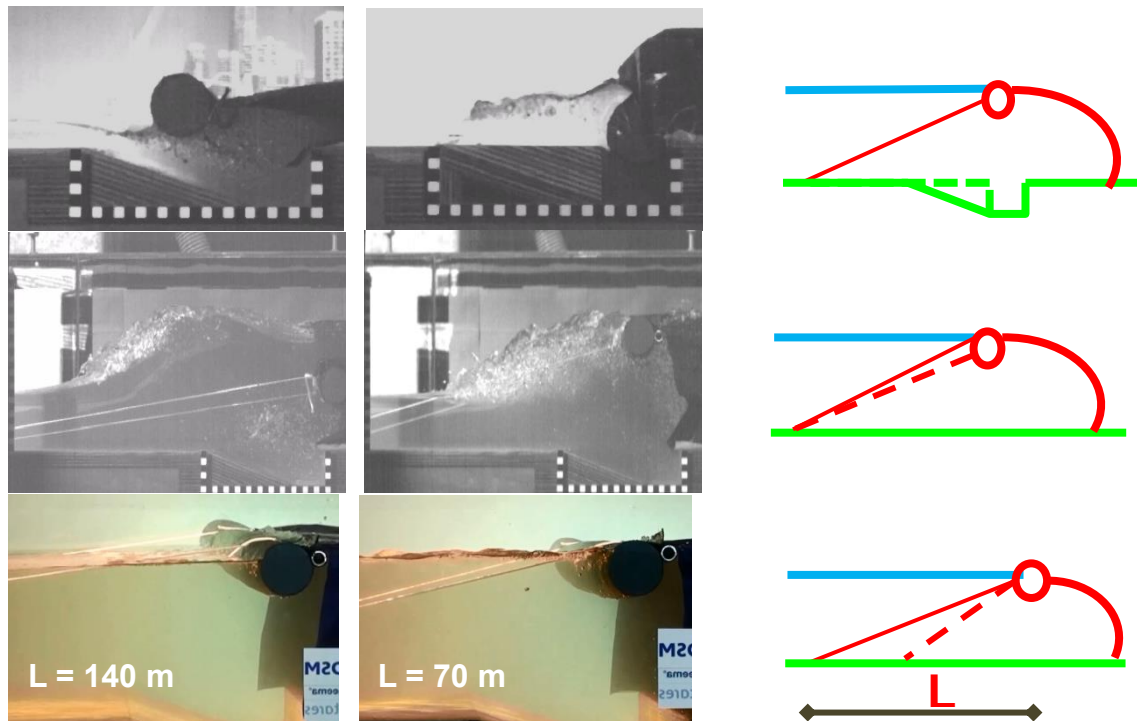


Figure 7. Various optimizations that were tested (dashed lines).

Extreme tsunami. Kato (2012) describes that tsunami structures should be tenacious, or resilient: that means that they should not collapse if the tsunami level exceeds the primary design level (Level I tsunami). This was tested by applying the (at least) 33 m high tsunami. As can be seen in Figure 8, the barrier remains erected, although forces on the membrane will increase.

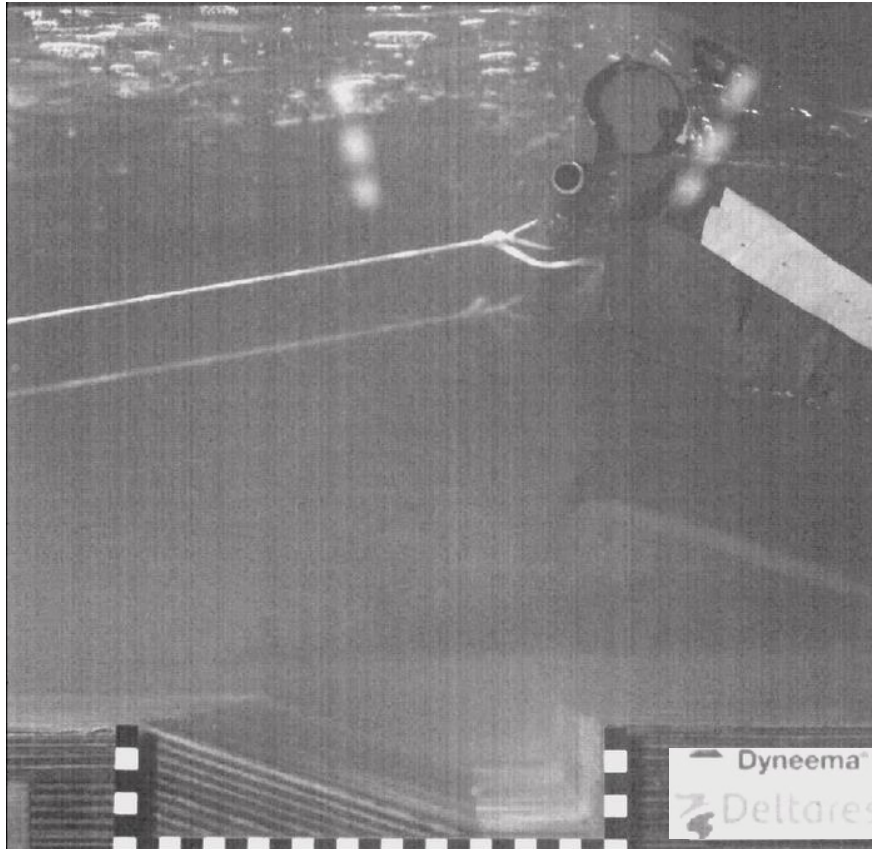


Figure 8. Tsunami of 33 m overflows the barrier (top right), which stays erected.

FORCES

The maximum total force of a bore impact typically is the hydrostatic water pressure of the reflected bore height, as seen in Ramsden & Raichlen (1990), from which some results are given in Figure 9. The largest pressures are found at the bottom of the wall at initial bore impact. However, the maximum total force occurs when the bore is just reflected, and it has a simple hydrostatic pressure distribution, so the total force is, as was assumed for the static case in the beginning of the paper:

$$F_{\max} = \frac{1}{2} \rho g H^2 \quad . \quad (4)$$

The typical maximum forces by (hydrostatic) pressure in the reflected wave are ≈ 2 MN/m for the 20 m high tsunami and ≈ 5 MN/m for the 35 m high tsunami (and 20 m high barrier).

It is expected that the floater and cavity will stop most direct debris impact at surface and bottom. Also the initial bore impact acts on the underside of the floater, and backside of the cavity which are embedded thoroughly in the ground. Other extreme forces are also expected to be damped somewhat by the flexibility of the membrane.

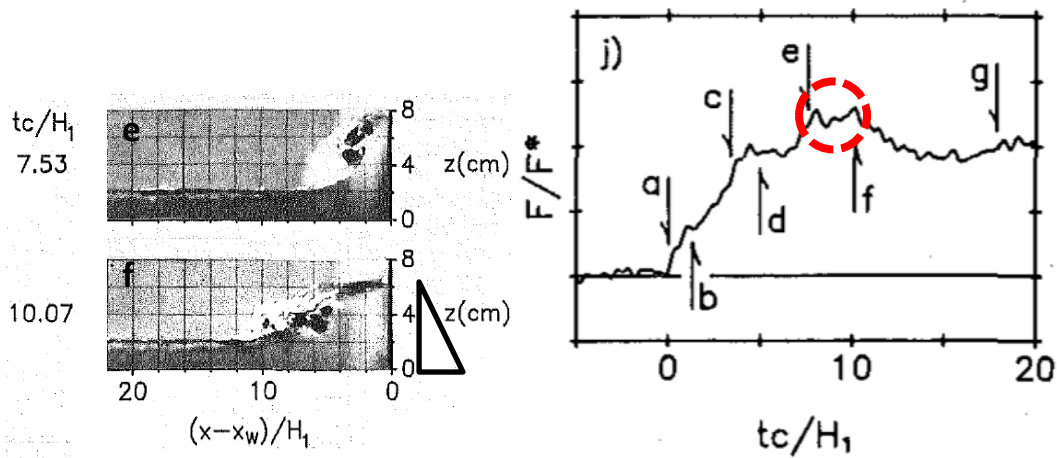


Figure 9. Impact force of bore impact on wall (Ramsden & Raichlen, 1990).

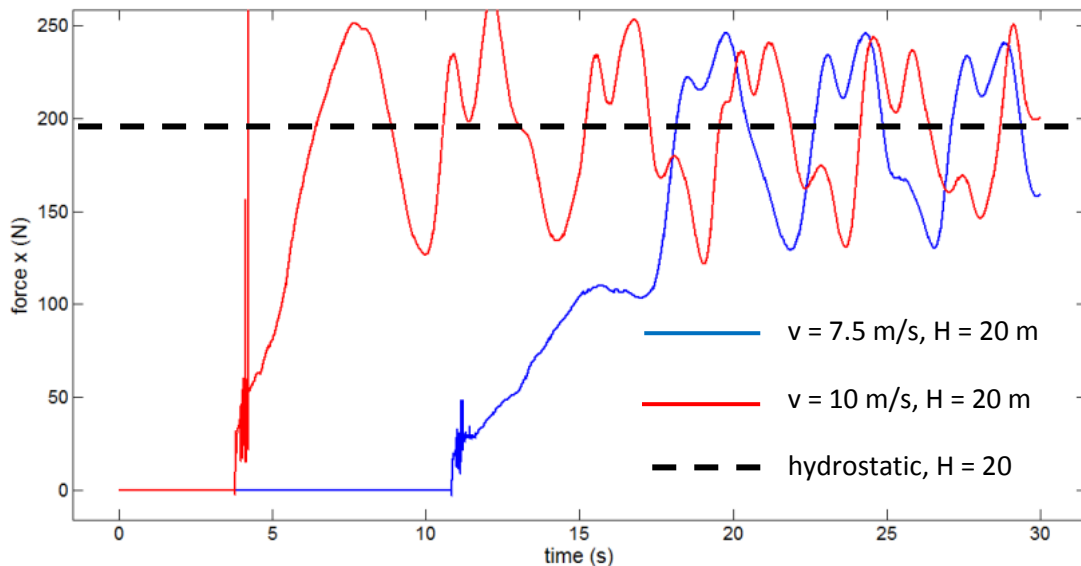


Figure 10. Calculated force during bore impact for two Comflow calculations.

CONCLUSIONS

Physical model tests were executed to verify that the tsunami barrier with Dyneema[®] would deploy under a tsunami attack. It was seen that the principle of the tsunami barrier works. The barrier concept is suitable for communities which should remain connected to the sea, but protected from devastating tsunamis.

A novel tsunami generating technique was applied in the tests, giving large velocity flow attack followed by a long (theoretically infinite) duration high water level. A 19 m high (reflected) tsunami, with a bore flow velocity of 7.5 m/s, was fully blocked by a flexible membrane barrier, in the 2D setup. For a 10 m/s approach flow, initially some water spilled over the barrier. With a much higher water level

($H > 33$ m) the barrier also remained erected, although some overflow occurred. Based on previously reported material characteristics a 50 m wide (cross shore) and 6 mm thick Dyneema membrane can withstand a 20 m high water level with a safety factor of 2.

Aspects like cable length and floater position can be optimized. Further study should improve the understanding of the possibilities of the barrier concept. Aspects that should be considered further are 3D effects (load concentration, irregular hydraulic attack), debris impact, foundation loads, side connection, tsunami characterization for a specific location (height, velocity), etc.

REFERENCES

- Arikawa, T., M. Sato, K. Shimosako, I. Hasegawa Gyeong-Seon Yeom and Takashi Tomita (2012) Failure mechanism of Kamaishi breakwaters due to the great east Japan earthquake tsunami. ICCE 2012
- Esteban, M., Jayaratne, R., Mikami, T., Morikubo, I., Shibayama, T., Thao, N., Ohira, K., Ohtani, A., Mizuno, Y., Kinoshita, M., and Matsuba, S. 2014. Stability of Breakwater Armor Units against Tsunami Attacks. *Journal of Waterway, Port, Coastal, and Ocean Engineering*, March 2014, Vol. 140, No. 2 : pp. 188-198
- Fulmi, Y., M. Nakamura, H. Shiraishi, Y. Sasaki (1963) Hydraulic study on tsunami. *Coastal Engineering in Japan*, Vol. 6.
- Goring and Raichlen (1980). The generation of long waves in the laboratory. International Conference on Coastal Engineering (ICCE) 1980.
- Kato, F., Suwa, Y., Watanabe, K. and Hatogai, S. (2012). Mechanism of Coastal Dike Failure Induced by the Great East Japan Earthquake Tsunami. Proc. of 33rd Int. Conf. on Coastal Engineering. Santander, Spain.
- Kimura, Y., Mase, H., Nakayasu, K., and Morii, T. (2014) Experimental Study on Real-Time Tsunami Protection Structures. *Journal of Waterway, Port, Coastal, and Ocean Engineering* 2014 140:3.
- Madsen, P.A., Fuhrman, D.R. & Schäffer, H.A. (2008) On the solitary wave paradigm for tsunamis. *J. Geophysical Research*, Vol 113, December 2008.
- Marissen, R. (2011) Design with Ultra Strong Polyethylene Fibers, *Materials Sciences and Applications*, Vol. 2, No. 5, 2011, pp. 319-330. <http://dx.doi.org/10.4236/msa.2011.25042>
- Marissen, R., Mulder, J. S., Wienke, D., Bergsma, O. (2013) Design Considerations on a Flexible Membrane Tsunami Flood Barrier. *Materials Sciences and Applications*, 2013, 4, pp. 846-855. <http://dx.doi.org/10.4236/msa.2013.412108>
- Ramsden J. D. and Raichlen F. (1990). Forces on vertical wall caused by incident bores. *Journal of Waterway, Port, Coastal, and Ocean Eng.* 116:5, p. 592-613
- Rossetto, T., W. Allsop, I. Charvet, D. I. Robinson. (2011) Physical modelling of tsunami using a new pneumatic wave generator. *Coastal Engineering*. Volume 58, Issue 6, June 2011, Pages 517–527.
- Tadepalli, Srinivas and Costas Emmanuel Synolakis. (1994) The run-up of N-waves on sloping beaches. *Proceedings: Mathematical and Physical Sciences* Vol. 445, No. 1923 (Apr. 8, 1994), p. 99-112. The Royal Society. <http://www.jstor.org/stable/52554>.